

Three-dimensional reconstruction of the pharyngeal gland cells in the predatory nematode *Pristionchus pacificus*

Metta Riebesell | Ralf J. Sommer 

Department for Evolutionary Biology, Max-Planck Institute for Developmental Biology, Spemannstrasse 37, Tübingen 72076, Germany

Correspondence

Ralf J. Sommer, Max-Planck Institute for Developmental Biology, Department for Evolutionary Biology, Spemannstrasse 37, 72076 Tübingen, Germany.
Email: ralf.sommer@tuebingen.mpg.de

Abstract

Pristionchus pacificus is a model system in evolutionary biology and for comparison to *Caenorhabditis elegans*. As a necromenic nematode often found in association with scarab beetles, *P. pacificus* exhibits omnivorous feeding that is characterized by a mouth-form dimorphism, an example of phenotypic plasticity. Eurystomatous animals have a dorsal and a sub-ventral tooth enabling predatory feeding on other nematodes whereas stenostomatous animals have only a dorsal tooth and are microbivorous. Both mouth forms of *P. pacificus*, like all members of the Diplogastridae family, lack the grinder in the terminal bulb of the pharynx resulting in a fundamentally different organization of several pharynx-associated structures. Here, we describe the three-dimensional reconstruction of the pharyngeal gland cells in *P. pacificus* based on serial transmission electron microscopical analysis of 2527 sections of 50 nm thickness. In comparison to *C. elegans*, *P. pacificus* lacks two gland cells (g2) usually associated with grinder function, whereas the three gland cells of g1 (g1D, g1VL, and g1VR) are very prominent. The largest expansion is seen for g1D, which has an anterior process that opens into the buccal cavity through a canal in the dorsal tooth. We provide the morphological description and fine structural analysis of the *P. pacificus* gland cells, the behavior of the pharynx and preliminary insight into exocytosis of gland cell vesicles in *P. pacificus*.

KEYWORDS

Caenorhabditis elegans, gland cells, pharynx, predatory feeding, *Pristionchus pacificus*

1 | INTRODUCTION

Pristionchus pacificus has emerged as a model system for integrative evolutionary biology that allows laboratory-based mechanistic studies to be linked to fieldwork (Sommer, 2015; Sommer, Carta, Kim, & Sternberg, 1996). Forward and reverse-genetic tools, including the CRISPR/Cas9 system for genetic engineering, are available in *P. pacificus*, and work as efficiently as in *Caenorhabditis elegans* (Witte et al., 2015). In addition, fieldwork in ecology and population genetics allow insight into the natural history of the organism, which, when combined with phylogenetic studies in the genus *Pristionchus* (Kanzaki, Ragsdale, Herrmann, & Sommer, 2014; Ragsdale, Kanzaki, & Herrmann, 2015) and the family Diplogastridae (Kanzaki & Giblin-Davis, 2015; Susoy, Ragsdale, Kanzaki, & Sommer, 2015), provides a comprehensive understanding of the biology of these nematodes. *Pristionchus pacificus* has a necromenic association with scarab beetles, such as the Oriental beetle *Exomala orientalis* in Japan and North America and the rhinoceros beetle

Oryctes borbonicus on La Réunion Island (Figure 1a) (Herrmann et al., 2007; Meyer et al., 2017; Morgan et al., 2012). On the living beetle, *P. pacificus* is found exclusively in the arrested dauer stage and exits the dauer stage only after the beetle's death to exploit the developing community of decomposers on the decaying carcass as food source (Meyer et al., 2017). This type of association represents one of several evolutionary scenarios that have resulted in an enormous radiation and diversity of entomophilic nematodes (Kanzaki & Giblin-Davis, 2015).

As a result, *P. pacificus* and many of its relatives are omnivorous feeders that can grow on bacteria, yeast, and other microbes (Rae et al., 2008; Sanghvi et al., 2016). In addition, however, *P. pacificus* is a predatory nematode that can kill and subsequently feed on larvae of other nematode species (Figure 1b) (Bento, Ogawa, & Sommer, 2010; Wilecki, Lightfoot, Susoy, & Sommer, 2015). Predatory feeding in this species is associated with a dimorphism in mouth morphology that represents an example of phenotypic plasticity (Figure 1e,f). Worms form teeth that occur in two alternative phenotypes. Eurystomatous (Eu)

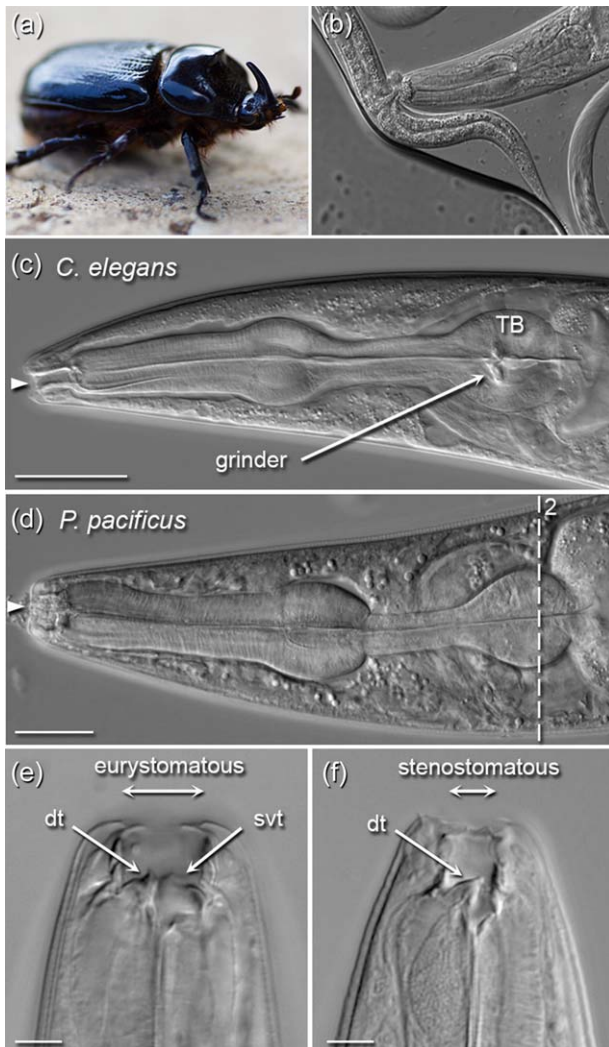


FIGURE 1 Characteristic life style features of the diplogastrid nematode *Pristionchus pacificus*. (a) *Oryctes borbonicus*, one of the scarab beetle hosts of *P. pacificus* on La Reunion Island. Image taken by Jan Michel Meyer. (b) *P. pacificus* adult predating on *C. elegans* larva. Image taken by Andreas Weller. (c, d) DIC micrographs of the pharynx region of *C. elegans* and *P. pacificus*. Left lateral view, central focal plane. Bars = 20 μm . The pharynx is a compact pumping organ separated from the pseudocoelom by a thick basal lamina. (c) The buccal cavity (arrowhead) of *C. elegans* forms a long, narrow tube without teeth for sucking in bacteria, the terminal bulb (TB) has a grinder (arrow) for crushing them, two traits typical of the purely bacterivorous species. (d) The buccal cavity (arrowhead) of the omnivore *P. pacificus* is wide and shallow with moveable teeth, the terminal bulb (TB) lacks a grinder. Dashed line indicates approximate section level of TEM cross-section shown in Figure 2. (e, f) DIC micrographs showing the mouth-form dimorphism in *P. pacificus*. Dorsal is to the left. Arrows indicate the width of the buccal cavity. Bars = 5 μm . Images from Sommer et al. (2017). (e) Eurystomatous mouth with a wide buccal cavity, a big, claw-like dorsal tooth (dt) and an opposing ambos-shaped sub-ventral tooth (svt), which can move forward for predatory feeding. (f) Stenostomatous mouth with a narrower and deeper buccal cavity, a small, flint-like dorsal tooth and no sub-ventral tooth, reflecting bacterivorous feeding habits

animals have a broad buccal cavity, a claw-like dorsal and an additional sub-ventral tooth, which together allow predation (Figure 1e) (Wilecki et al., 2015). The alternative stenostomatous (St) form has a narrow buccal cavity and a single flint-like dorsal tooth without sub-ventral counterpart, restricting its diet to microbes (Figure 1f). As mouth-form plasticity is irreversibly specified in individual worms, but contains elements of stochastic regulation in populations grown in fixed environments, *P. pacificus* mouth-form development became a genetic model to study the regulation of plastic traits (Serobyán & Sommer, 2017; Sommer et al., 2017). In short, genetic screens identified the *eud-1*/sulfatase and the nuclear hormone receptor *nhr-40* as developmental switches controlling mouth-form plasticity (Kieninger et al., 2016; Ragsdale, Müller, Rödelsperger, & Sommer, 2013). Recent studies identified an epigenetic level of mouth-form regulation that at least in parts occurs at the level of the *eud-1* switch gene (Serobyán et al., 2016). Together, the development of moveable teeth, predatory feeding, and mouth-form plasticity represent derived characters specific to *P. pacificus* and its relatives that are unknown from *C. elegans*. Therefore, the available molecular and genetic tools allow unprecedented insight into the regulation of the mouth form and its plasticity.

The facultative predatory life style of *P. pacificus* and other members of the Diplogastridae has resulted in a number of morphological adaptations that define the distinctive pharynx of this family: most importantly, moveable teeth are present in the stoma and the typical grinder for crushing bacteria that is found in the terminal bulb of the pharynx in Rhabditidae (Figure 1c) is absent (Figure 1d) (Rae et al., 2008), while outwardly the typical three-part pharynx known from all free-living nematodes of the order Rhabditida consisting of corpus, isthmus, and terminal bulb (TB) has been kept. Previous studies have indicated that the absence of the grinder is also known from other taxa of the order Rhabditida, but Diplogastridae are the only group that is not parasitic (Fürst von Lieven, 2003). The countless variations of the nematode pharynx and its gland cells have been described in the comprehensive monographs of Chitwood and Chitwood, (1950), Maggenti (1981), Bird and Bird (1991) and others. Most importantly, however, the work of Baldwin and coworkers has systematically investigated the ultrastructure of the pharynx in *Zeldia punctata* (Cephalobida), *Diplenteron* sp. (Diplogastridae; *Diplenteron* is now called *Mononchoides*), and the distantly related *Teratocephalus lirellus* (Teratocephalidae), the latter of which can be considered as outgroup (Zhang and Baldwin, 1999, 2000, 2001). These studies indicate that the number of gland cells varies between three and five and based on the phylogenetic position of *Teratocephalus*, the three-gland cell pattern might represent the plesiomorphic (ancestral) condition (Zhang & Baldwin, 2001). However, such interpretations have to be considered with care, because convergence between major taxa has also been discussed (Zhang & Baldwin, 2000). In addition to these descriptive and phylogenetic studies on pharyngeal ultrastructure, Fürst von Lieven was the first to investigate the functional morphology of the pharynx with a strong focus on several members of the Diplogastridae (Fürst von Lieven, 2002, 2003). Nonetheless, the best understood pharynx is still that of the model organism *Caenorhabditis elegans*. Based on the pioneering description

by Albertson and Thomson (1976), numerous aspects of the feeding behavior have been intensively studied in *C. elegans* (Avery & Thomas, 1997) and we will, therefore, use *C. elegans* as reference point in our study.

Previous studies in *P. pacificus* have investigated the consequences of the adaptations to predatory feeding for the pharyngeal nervous system. Surprisingly, the cellular composition of the pharyngeal nervous system is identical between *P. pacificus* and *C. elegans* although the neural wiring shows large differences (Bumbarger, Riebesell, Rödelberger, & Sommer, 2013). Here, we extend the analysis of feeding- and predation-associated morphological structures in *P. pacificus* by investigating the pharyngeal gland cells by transmission-electron-microscopy (TEM)-based reconstruction. This three-dimensional reconstruction of the pharyngeal gland cells in *P. pacificus* provides a comparative framework for functional studies of nematode predation and omnivorous feeding.

2 | MATERIALS AND METHODS

2.1 | TEM reconstruction

For the reconstruction of the pharyngeal gland cells in *Pristionchus pacificus* Sommer et al. (1996), we made use of a set of 3000 serial TEM sections of 50 nm thickness covering the anterior part of a high-pressure-frozen and freeze-substituted eurytomatous adult hermaphrodite of strain PS312, a second set of 2762 serial sections was used for reference and cross checking. The generation of the original datasets is described in Bumbarger et al. (2013) and in greater detail in protocol 9 of the *Pristionchus pacificus* protocols in WormBook (Pires-daSilva, 2013). The segmentation was done manually in TrakEM2 (Cardona et al., 2012) and the visualization in Blender 2.71. To clarify certain morphological features we referred to TEM micrographs from our archive of past preparations of very similarly processed worms of the same strain. Comparisons to the well-studied model organism *C. elegans* as a representative of the Rhabditidae are based on information provided in the pharynx chapter of the *C. elegans* Atlas (Altun & Hall, 2008), WormImage (www.wormimage.org), the original literature and own observations.

2.2 | Fluorescent staining of pharynx muscles

Whole worms were washed three times in PBS to remove bacteria, fixed in 3.7% formaldehyde (FA) in Na₂HPO₄ for three hours (RT) with gentle rocking. The FA solution was removed and worms were washed in fresh PBS three times for 30 min. Then, samples were extracted with acetone (−20°C) for 2 min. After removal of acetone, worms were re-hydrated in three washes of PBS for 30 min each. To stain actin filaments, worms were incubated in fluorescently labelled phalloidin at a concentration of 0.15 μM in PBS (AlexaFluor® 546 Phalloidin A-22283, Molecular Probes) for three hours on a rotating wheel in the dark. After three final washes in PBS of 30 min. each, worms were mounted in VectaShield (H-1000, Vector Laboratories, Inc.) on a 4% agar in water pad and inspected with a Zeiss Axio Imager.Z1 using a

Spot camera, model 9.0 monochrome-6 and Metamorph software 6.1. Images were subsequently processed by 20 iterations of deconvolution (AutoDeblur & AutoVisualize 9.1).

3 | RESULTS

3.1 | *Pristionchus pacificus* has three massive pharyngeal gland cells

In nematodes of the group formerly known as the class of Secernentea, the TB accommodates a total number of either five or three pharyngeal gland cells (Maggenti, 1981; Zhang & Baldwin, 2001). In *P. pacificus* we found three pharyngeal gland cells of the g1 class, one located dorsally (g1D) and two sub-ventrally (g1VL, g1VR; Figures 2 and 3; Supporting Information Movie S1). *Pristionchus* g1 is homologous with *C. elegans* g1 in number and position of orifices. In contrast, the second class of gland cells present in *C. elegans*, g2, with a left and a right ventral gland opening into the pharyngeal lumen just anterior of the grinder, is absent in *P. pacificus* as is the grinder. The same is true for most of the muscle filaments that drive the grinder machinery in *C. elegans*. The space occupied by grinder, grinder musculature and grinder-associated g2 in *C. elegans* is taken up by greatly enlarged g1 cell bodies in *P. pacificus*. Thus, the TB of *P. pacificus* can be described as glandular (without grinder) rather than muscular (with grinder) as in *C. elegans* with a presumed shift from mechanical to enzymatic break up of bacteria. The same was observed in the diplogastrid nematode *Diplenteron* sp. analyzed by Zhang and Baldwin (1999).

The dominance of the g1 glands and their complex shape become obvious in the TEM cross section through the posterior TB shown in Figure 2a (for more sections at different levels see Figure 3e,f and Supporting Information Figures S1–S4). Each of the three massive g1 cell bodies occupies one of the three sectors formed by the two sub-dorsal and the ventral marginal cells (mc3). While the ventral glands remain largely confined to their sectors, g1D crosses the sector borders on both sides expanding deeply into the sub-ventrally adjoining territories of the g1V cells, thus gaining in volume at the expense of the sub-ventral glands (Figures 2a and 3d,f). These observations hint at a special role of the dorsal gland cell. In the second specimen g1D is also bigger, but the difference is not quite as pronounced suggesting variability between specimens.

Within the sectors the gland cells share space with muscle and neuronal cell bodies and their extensions. In particular, they wrap around each of the scarce muscle fiber bundles of pharyngeal muscle cell 6 (pm6), which connect the pharyngeal lumen to the basal lamina and are responsible for opening and closing the lumen (Figures 2a and 3f; Supporting Information Figure S3A). As a result, the gland cells appear to be pierced by the filament bundles in cross-sections. Similarly, the processes of the I4 and I5 neurons pass through the gland cells in deep infoldings of the gland plasma membrane in the small commissure in the anterior TB (Bumbarger & Riebesell, 2015). In regions of the TB where marginal and muscle cells retract inwards toward the pharyngeal lumen and in places

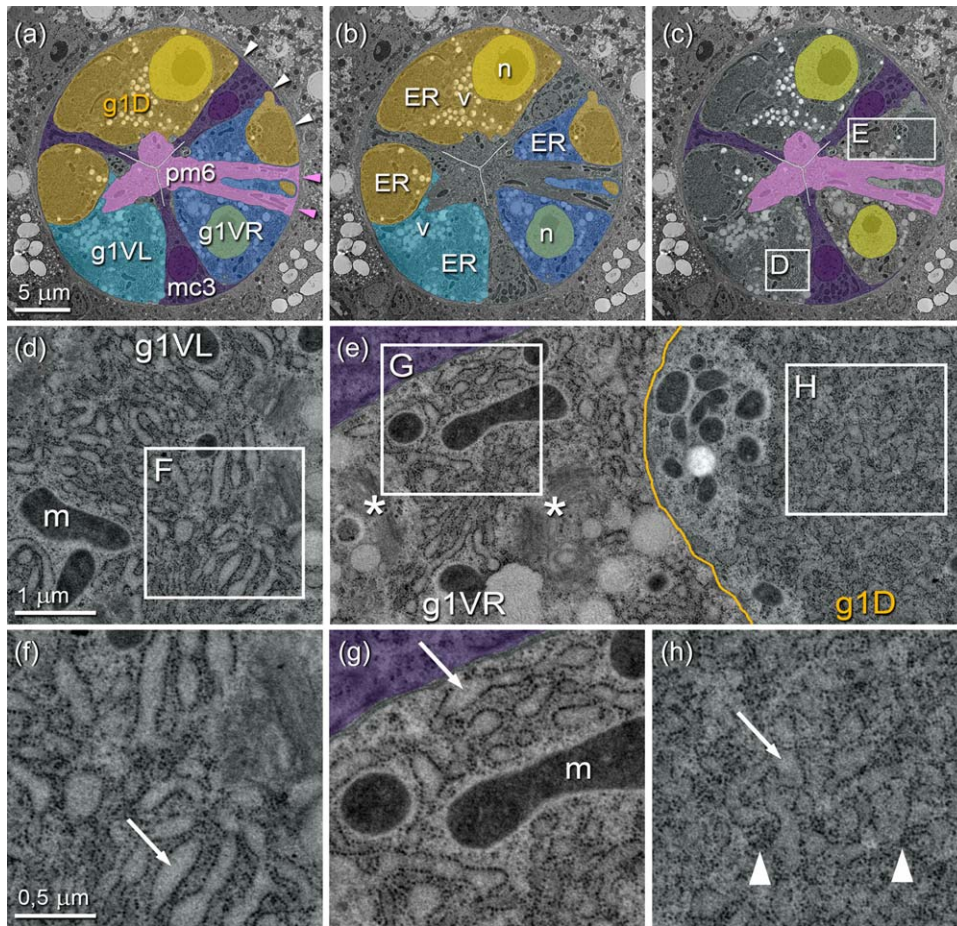


FIGURE 2 *Pristionchus pacificus*, ultrastructure of the pharyngeal gland cells in Transmission electron micrographs of a cross-section through the posterior central part of the terminal bulb (TB) of the pharynx at the level of the g1D nucleus; for approximate plane of sectioning see dashed line in Figure 1d. Compare to Supporting Information Figure S3. (a–c) Three gland cells (g1), three muscle cells (pm) and three marginal cells (mc) form the monolayered pharyngeal epithelium in the TB. They are highlighted in different colors: g1D (ochre), g1VL (light blue), g1VR (dark blue), g1 nuclei (yellow), pm6 (pink), mc3 (dark purple), mc3 nuclei (reddish purple). Bar 5 μm . (a) Gland, muscle and marginal cells are false-colored. The marginal cells divide the pharynx into a dorsal and two sub-ventral sectors, which harbor the cell bodies of the three gland cells. The dorsal gland is so massive that it wraps around the mc and expands into both sub-ventral sectors. The central space close to the triradiate pharyngeal lumen is occupied by the cell bodies of pm6. Here, pm6VR sends a bundle of radially oriented myofilaments to the outer plasma membrane piercing g1VR. Arrowheads point at the basal lamina, whose inner surface serves as muscle attachment point (pink arrowheads) and whose outer surface isolates the pharynx from the rest of the body cavity (white arrowheads). (b) Only the gland cells are highlighted to demonstrate the dominance of this cell type in the TB. Gland nuclei (n) are large with large nucleoli. The g1D nucleus has its full size, the g1VR nucleus is smaller because it is a lateral section, the g1VL nucleus is more posterior. The cytoplasm is filled with rough ER (ER) and vesicles (v). (c) Gland cells without color overlay to show the clear differences in cytoplasmic structure between dorsal and ventral glands. The prominent organelles are rough ER and aggregations of electron-light secretory vesicles. In g1D the ER region appears finer and slightly more electron-dense. The extreme electron-lightness of the g1D vesicles could be an artifact. In g1V the ER regions appear coarser and more electron-light while the vesicles are more electron-dense. (d–h) Details at two higher magnifications. White boxes in c indicate the areas enlarged in d and e. White boxes in d and e show the areas enlarged in panels f, g, and h directly underneath. m = mitochondria, asterisk = Golgi apparatus, not well-preserved. (d + f; e left + g) The coarse appearance of the g1V cytoplasm is caused by larger, more elongated and more clearly delineated ER cisternae with dilated lumen and electron-lighter material inside (arrows). The overall ribosome density appears to be lower. (e right + h) The finer appearance of g1D cytoplasm to the right of the yellow line is due to smaller, more rounded ER cisternae with more electron-dense material inside the lumen (arrow) and a higher density of unbound ribosomes (arrowheads)

where the dorsal gland has crossed over into the sub-ventral sector, the neighboring gland cells form direct contacts with each other unless the presence of other cell classes prevents this (Supporting Information Figure S1A). The contact zones between them are winding and overlapping. The full complexity of the outline of the inner surfaces and the contact zones is best seen in a posterior

view (Figure 3d) and in the animated three-dimensional reconstruction with single rotating gland cells (Supporting Information Movie S1). Taken together, the three gland cells in *P. pacificus* have cell bodies of enormous size and highly complex shape because of their tendency to fill out the entire space between the other cells of the TB.

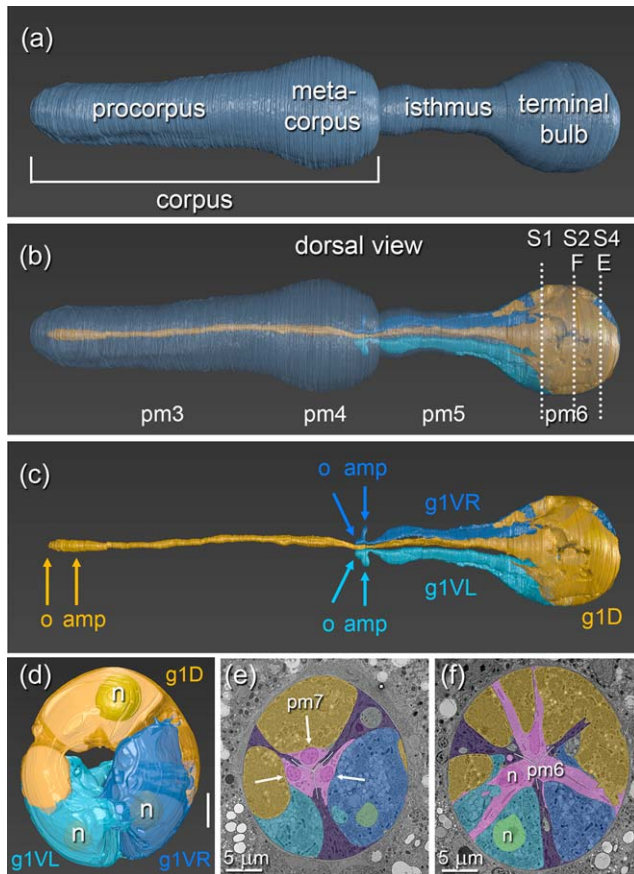


FIGURE 3 *Pristionchus pacificus*, location and morphology of the pharyngeal gland cells. (a–d) 3D-reconstruction from a series of 2527 TEM cross-sections. (a–c) Dorsal view, anterior to the left. (a) Pharynx outline showing the compact shape of the organ, which is separated from the surrounding pseudocoelom by a thick basal lamina, and its typical division into corpus, isthmus and terminal bulb. The corpus is further subdivided into procorpus and metacarpus. (b) Dorsal view of the pharynx showing the location of the gland cells within the semitransparent pharynx outline. The position of the main pharyngeal muscle segments is indicated: pm3 in procorpus, pm4 in MC, pm5 in isthmus, pm6 in TB. Dotted lines refer to transverse sections e and f and Supporting Information Figures S1, S2 (identical with f) and S4 (identical with e) (c) The massive cell bodies of the three g1 gland cells are located in the terminal bulb. The dorsal gland (g1D) sends out a long anterior process, which opens (o) into the buccal cavity through the dorsal tooth. The anterior tip of the process is wider and serves as collecting reservoir or ampulla (amp) for secretory vesicles. The two ventral glands (g1VL, g1VR) have shorter processes with openings (o) into the pharyngeal lumen at the posterior of the metacarpus. The fin-like protrusions just behind the openings are the ampullae (amp). (d) Posterior view of the pharyngeal glands showing the position of the nuclei (n) and how the three cells overlap. Bar = 5 μ m (e, f) TEM cross-sections with false-color overlays as in Figure 2a. Planes of sectioning are indicated as dotted lines in Figure 3b. Bars = 5 μ m (e) Cross-section through the degenerated pm7 segment in the posterior terminal bulb showing pm7 nuclei and cell bodies at their largest extent (arrows). In comparison to pm6 shown in panel f the cells are greatly reduced in size, do not contain any myofilaments and do nowhere reach the basal lamina. (f) Cross-section through central terminal bulb. In this position, all three pm6 cells show myofilament bundles connecting the cuticle inside the lumen of the pharynx to the basal lamina on its outer surface. At contraction of the myofilaments the lumen will open and assume a triangular shape. Two pm6 nuclei and the g1VL nucleus are visible (n)

3.2 | Different fine structure of g1D and g1V cells

Fine structure analysis of the three pharyngeal gland cells suggests a special role of the g1D cell. The TEM cross-sections (Figure 2, Supporting Information Figures S1–S4) reveal that the g1 cell bodies possess all the typical characteristics of highly active secretory cells: large nuclei with large nucleoli, an elaborate network of rough endoplasmic reticulum (rER) densely studded with ribosomes, numerous Golgi complexes (Supporting Information Figure S4G), membrane-bound secretory vesicles of all sizes, and a large number of mitochondria. For *C. elegans* it is known that g1 and g2 differ in the appearance of their vesicles and in the structure of their cytoplasm, which was described as “lamellar” for all g1 cells and as “rather clear” for g2 (Albertson & Thomson, 1976; Altun & Hall, 2008). In contrast, obvious cytoplasmic differences between dorsal and ventral g1 cells in *C. elegans* could not be detected in the images available. Interestingly, however, this is exactly what we find in *P. pacificus* and also when looking at the TEM micrographs of *Diplenteron* in Zhang and Baldwin (1999). While g1V is conserved with *C. elegans* in its “lamellar” appearance, g1D exhibits a much finer, smoother and seemingly more uniform texture (Figure 2).

At higher magnification it becomes clear that the difference in appearance is caused by a distinct morphology of the cisternae of the rER. In the dorsal gland, the rER cisternae tend to be smaller and rounder with electron-denser contents while in the ventral glands, they tend to be larger, more elongated and more dilated with contents that is less electron-dense and produces a stronger contrast to the attached ribosomes, just as in *C. elegans* (Figure 2d–h; Supporting Information Figures S1D–I–S4D–I). Especially when multiple g1V cisternae are found in parallel orientation (Supporting Information Figure S4E,F,H,I), the cytoplasm assumes a characteristic lamellar appearance. Another reason for the different appearance of the dorsal g1 seems to be a higher density of unbound ribosomes between the cisternae. Thus, the finer texture of the dorsal gland with narrower cisternae, electron-denser contents and higher density of unbound ribosomes is a special trait, an internal differentiation, which may indicate distinct functions in connection with the dorsal tooth and predation. Similarly, the appearance of the secretory vesicles in the dorsal gland differs from that in the sub-ventral glands in electron density, texture and shape.

3.3 | Three-dimensional reconstruction of the pharyngeal gland cells

Next, we performed a three-dimensional reconstruction, which allows an outside view of the entire pharynx and the gland cells. The reconstructed pharynx outline (Figure 3a) shows the typical three-part pharynx of the free-living nematodes of the order Rhabditida consisting of corpus, isthmus, and terminal bulb (TB). As in most free-living representatives of the order, the corpus is subdivided into procorpus and metacarpus (MC) (Fürst von Lieven, 2003). The basal surface of the pharynx is surrounded by a thick basal lamina, which externally separates the compact organ from the pseudocoelom (Figures 1c,d and 2a, arrowheads) and internally serves as attachment point for the pharyngeal muscles (Figure 2a, pink arrowheads) (Fürst von Lieven, 2003). The

pharynx functions as an autonomous pumping unit under the control of the pharyngeal nervous system, with the connection to the somatic nervous system mediated merely by a bilateral pair of gap junctions between I1 and the somatic interneuron RIP (Bumbarger & Riebesell, 2015; Bumbarger et al., 2013).

The semi-transparent view (Figure 3b) reveals the position of the gland cells within the pharynx: the large cell bodies with irregular surfaces in the TB and the anterior processes in isthmus and corpus. In the transition zone between TB and isthmus, the gland cell bodies gradually narrow into long processes extending anteriorly within the pharyngeal nerve cords toward their respective sites of secretion (Figure 3c arrows). The ventral processes open into the pharyngeal lumen in the posterior MC, while the dorsal process travels all the way to the mouth in exactly the same way as in *C. elegans*.

At the entry point into the MC, the gland processes have to pass a narrow constriction at the border between the pm5 and pm4 muscle segments. Here, the processes become very thin and move to the center (Figure 3b,c, Supporting Information Figure S5A,B). Before opening into the lumen of the pharynx the sub-ventral processes form fin-like ampullae, which presumably serve as collecting reservoirs for secretory vesicles (Figure 3c arrows; Supporting Information Figure S5C). The

ampulla of g1D is a simple swelling of the process in dorso-ventral direction so that it is not visible in the dorsal view in Figure 3c. For a lateral view we refer to the DIC image in Figure 4a, which shows the ampulla with a mass of vesicles stored behind the dorsal tooth, through which g1D opens into the buccal cavity (Figure 4a,c).

3.4 | The opening of the glands and observations on exocytosis

Next, we investigated the gland cell ampulla in more detail to understand how the future secretions of the gland cell vesicles reach their destination (Figure 4; Supporting Information Figure S5). The anterior ends of the gland cell processes of *P. pacificus* do not open into the pharyngeal lumen directly but via short cuticular ducts, similar to what is known from other nematodes (Altun & Hall, 2008; Munn & Munn, 2002). These cuticular ducts exhibit blind, distal ends that are embedded in the tips of the processes and proximal ends that are continuous with the cuticle of the lumen (Supporting Information Figure S5C). The ducts seem to be extensions of the luminal cuticle connecting to the gland cells. In *P. pacificus*, the ducts of the ventral glands open directly into the lumen (Supporting Information Figure S5C), whereas the duct of the dorsal gland opens into the buccal cavity through a canal in the

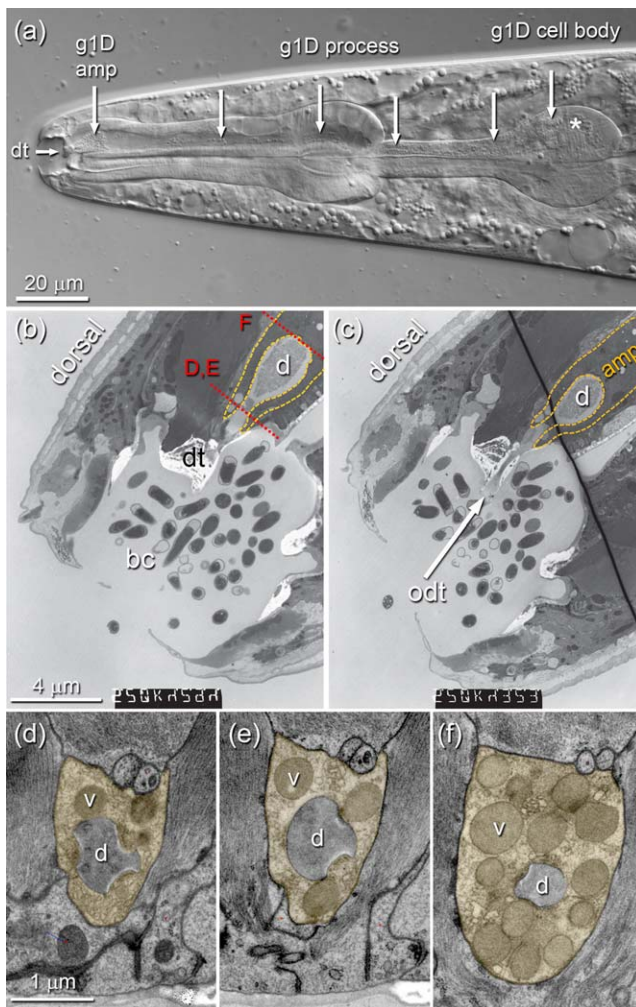


FIGURE 4.

FIGURE 4 *Pristionchus pacificus*, the dorsal gland cell g1D and its orifice. (a) DIC micrograph of the head region, left lateral view, central focal plane. The pharynx is the prominent organ, clearly delineated from the surrounding tissues. In the dorsal part of the pharynx g1D is easily detectable by its numerous secretory vesicles. Arrows indicate its extension from the cell body in the TB to its opening in the dorsal tooth (dt). The ampulla (amp) is half filled with vesicles. The asterisk indicates the position of the nucleus in a more lateral focal plane. (b, c) Longitudinal TEM micrographs through the buccal cavity (bc), left lateral view, taken in two slightly different focal planes. Enclosed in the anterior tip of the g1D process (yellow dashed line) is a short cuticular duct (d), which connects to the buccal cavity through an opening (o) in the dorsal tooth (dt). The common surface of gland cell process and duct is where the secretory vesicles are bound to release their contents into the lumen of the duct. The ampulla (amp) is full of vesicles (hard to see), the lumen of the duct shows some precipitate, which could be excreted material from the gland. Thick cuticular structures such as teeth are electron translucent and appear white. The buccal cavity is filled with bacteria. (d-f) TEM micrographs of transverse sections through the g1D process (yellow) in the region of the cuticular gland duct (d), the expected site of exocytosis. For approximate positions see red dotted lines in (b). As d and e are only about 250 nm apart, they share the dotted line. The g1D cytoplasm contains membrane-bound secretory vesicles (v) and surrounds the duct (d). The outline of the duct shows characteristic indentations, which are lined with electron-translucent material, supposedly chitin, on the inside. In some places electron-dense material is found on the outside. (d) A vesicle (v) in contact with the duct (d), which could be an initial phase of exocytosis. (e) Two vesicles in contact with the duct with electron-dense material in the contact zone, which could be the docking stage of exocytosis. (f) Section through ampulla (amp) near the posterior end of the duct showing many vesicles, one near the membrane bordering the duct

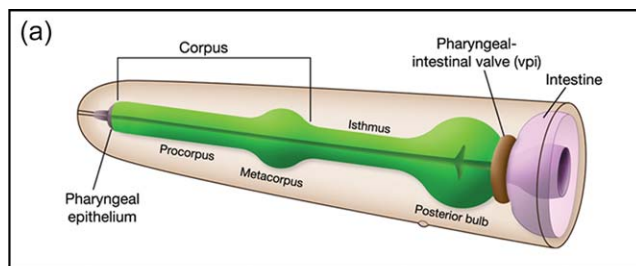
dorsal tooth (Figure 4b,c). The latter presents another special trait connected to predatory feeding. Food items too big to swallow are ripped open with the moveable predatory tooth and the content is sucked out (Figure 1b). The hollow tooth may allow the injection of required enzymes directly into the prey even before ingestion. In *P. pacificus*, the hollow tooth occurs in both mouth-forms, irrespective of their different feeding habits (Bumbarger et al., 2013; Ragsdale et al., 2013). Similar gland openings in dorsal teeth were recorded for several other diplogastrid species with claw-like dorsal teeth by Zhang and Baldwin (1999) and Fürst von Lieven and Sudhaus (2000).

Next, we tried to investigate where and how the content of the membrane-bound secretory vesicles is released into the ducts. It is only in the small zone of contact between gland cell process and enclosed gland cell duct that secretion by exocytosis can take place (Figure 4b,c; Supporting Information Figure S5C). Here, the duct has a characteristic shape in cross-sections with rounded indentations that may serve as docking sites for vesicles (Figure 4d-f; Supporting Information Figure S5B). Judging by the degree of electron-translucence, the thickness of the duct cuticle is greater in the indented regions and dense material is found on the gland cell side. After careful inspection of our transmission electron microscopy data we only found a few

instances in the dorsal gland cell process of one specimen which in all likelihood show secretory vesicles in the initial phase of exocytosis (Figure 4d-f). In Figure 4e, two vesicles are seen in close contact to the plasma membrane with electron dense material assembled at the site of contact, which may represent the docking stage. In Figure 4d, one vesicle appears to have fused with the membrane. We assume that exocytosis is fast and only triggered when needed so that the fact that we rarely observed it in high-pressure-frozen specimen, which were without food for some time prior to freezing, is not at all surprising.

3.5. | Behaviors of the pharynx

In addition to the described anatomical traits, diplogastrids also show a set of special pharyngeal behaviors. According to Chiang, Steciuk, Shtonda, and Avery (2006) the ancestral behaviors of the three muscle groups of the pharynx in free-living soil nematodes (Figure 5b) are (i) pumping of the corpus, (i.e., simultaneous contractions that open the lumen to suck in food particles), (ii) peristalsis of the isthmus, (i.e., a posteriorly directed wave of contractions that transports particles to the TB), and (iii) pumping of the TB, (i.e., simultaneous contractions that crush the particles when operating the grinder and pass them into the intestine). It is thought that originally, each of these three behaviors occurred independently from each other (Chiang et al., 2006). Divergence from this ancestral pattern occurred in several lineages but did not affect the corpus in free-living soil nematodes. In this group, corpus



(b)

Muscle Group	Corpus	Isthmus	Terminal Bulb	Grinder
Ancestral	pumping	peristalsis	pumping	+
Rhabditidae	pumping >	< pump. > peristal.	< pumping	+
Diplogasteridae	pumping	peristalsis >	< peristalsis	-
Evolution	conserved	evolving	evolving	

(c)

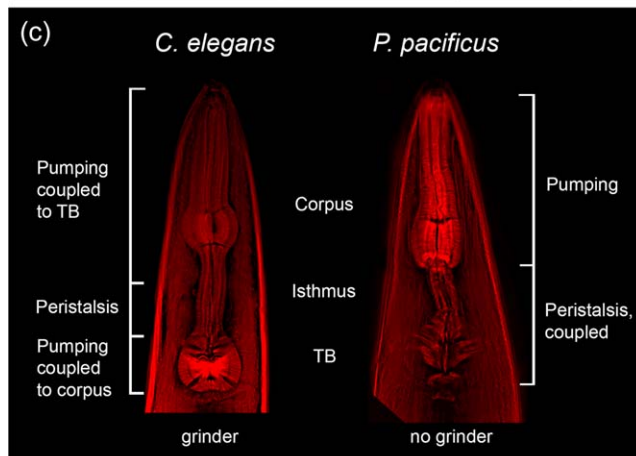


FIGURE 5.

FIGURE 5 Differences in pharyngeal behaviors between *C. elegans* and *P. pacificus*, (a) Graphic rendition of the *C. elegans* pharynx labeling the three muscle groups responsible for the functioning of the pharynx in the uptake and transport of food particles: corpus, isthmus, and posterior or terminal bulb (TB). (Reprinted from WormAtlas (wormatlas.org) with permission by Zeynep Altun MD, PhD and David Hall, PhD) (b) Table of changes in the behaviors of the different pharyngeal muscle groups during evolution according to Chiang et al. (2006). Pumping means near-simultaneous contraction and relaxation of all radially oriented muscle fibers, peristalsis means an anterior-to-posterior wave of contraction and relaxation. Angle brackets <> indicate that the behavior of a muscle group is coupled to the same behavior in another muscle group in the given direction. The ancestral situation consists of corpus pumping (red), isthmus peristalsis (blue), and TB pumping (orange), each happening independently of the other. In Rhabditidae the anterior isthmus has switched from peristalsis to pumping, coupled to corpus and TB pumping. In Diplogasteridae the TB does not have a grinder and switched from pumping to peristalsis, coupled to isthmus peristalsis. (c) Actin staining illustrating behavioral differences between the pharyngeal muscle groups. In *C. elegans* the strongest staining occurs in the muscles that drive the grinder machinery in the TB (pm6 and specifically pm7). Chiang et al. (2006) claim that in addition to the muscular corpus also the anterior part of the isthmus has assumed pumping function in *C. elegans*, but this difference between the pumping and peristaltic part of the isthmus is hard to see in our staining. In *P. pacificus* strong staining indicating pumping behavior is restricted to the corpus. Isthmus and TB show a weaker signal indicative of peristalsis. According to TEM evidence (Figure 3e) all of the radial bundles of actin filaments that are visible in the TB belong to pm6, pm7 does not contain myofilaments.

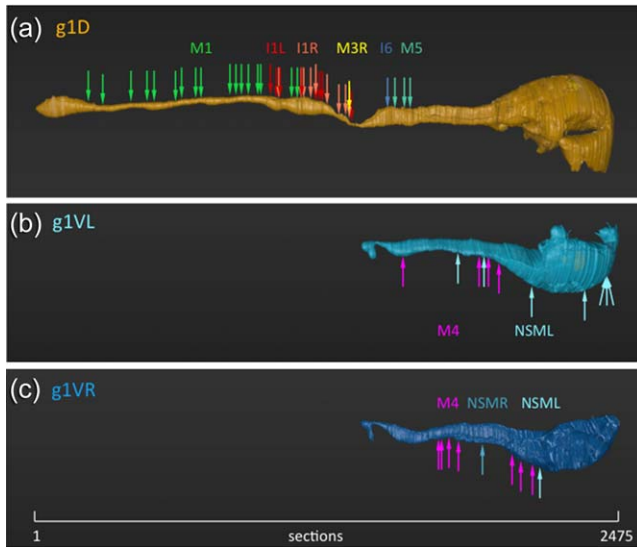


FIGURE 6 *Pristionchus pacificus*, innervation of the three pharyngeal gland cells of specimen 107 based on the connectivity data (Bumbarger et al., 2013). (a–c) The g1 cells are shown separately: g1D in lateral view, g1VL and g1VR were each slightly turned ventrally until the process appeared in its full width. Each of the seven neuron classes that synapse onto the glands is given a different color. If there is a left and a right neuron of the same class, the colors are similar but distinct. Each synapse is represented by an arrow. The anterior-posterior distribution is to scale. (a) In g1D all synapses are on the dorsal side as the neurons run on top of the gland process in the groove of the muscle cells. (b, c) In the ventral glands the position of the synapses is much more variable so that the arrows here merely indicate the anterior-posterior position. The section number for each synapse and the complete connectivity list including the adjacent output cells in double or triple synapses for this specimen are given in Table 1, for the second specimen in Table 2

pumping remained conserved, whereas the behaviors of isthmus and TB underwent considerable changes correlated to the evolution of feeding strategies: In Rhabditidae, for example, the anterior part of the isthmus joins in the pumping and the pumping motions of corpus, anterior isthmus and TB are coupled. In Diplogastridae, the TB lost its pumping behavior and switched to peristalsis, which became coupled to isthmus peristalsis (Chiang et al., 2006) (Figure 5b).

The difference between pumping segments with strong muscle activity and regions of peristalsis with weaker muscle activity is demonstrated in the actin staining shown in Figure 5c. In *C. elegans*, the grinder muscles in the TB (pm6 and pm7) show the strongest staining, whereas in *P. pacificus* the muscles of the procorpus (pm3) and particularly the metacarpus (pm4) stain most strongly. The TB muscles are reduced to a few randomly arranged bundles in pm6 (see also Figure 3f) while pm7 does not stain for actin at all in *P. pacificus*. TEM cross-sections (Figure 3e) confirm that pm7 has completely lost its functionality as a muscle cell. Although the three nuclei are well developed and located in the expected position, the cell bodies have drastically shrunk in size, lost their myofilaments, are no longer connected to the basal lamina (compare Figure 3e,f), and do not receive any synaptic input

TABLE 1 Gland cell innervation of *P. pacificus* specimen 107

Section #	Presynaptic neuron -> postsynaptic cells	Synapse ID
220	M1->pm3D+g1D	38846
282	M1->e3D+I3+g1D	38851
403	M1->pm3D+g1D	38828
470	M1->pm3D+g1D	38855
497	M1->pm3D+g1D	38857
591	M1->pm3D+g1D	38866
616	M1->pm3D+g1D	38868
675	M1->pm3D+g1D	38870
698	M1->pm3D+g1D	38872
821	M1->pm3D+g1D	38982
847	M1->pm3D+g1D	38986
867	M1->pm3D+g1D	38988
899	M1->pm3D+g1D	38990
938	M1->g1D+I3	38994
951	M1->pm3D+g1D	38996
993	I1L->g1D+I5	39591
1019	I1L->I1R+g1D	39096
1028	I1R->I1L+g1D	39094
1034	I1L->I5+I1R+g1D	39587
1082	M1->pm3D+g1D	39090
1107	M1->I3+g1D	38998
1122	I1R->e3D+g1D	39088
1125	I1L->I1R+g1D	39086
1133	I1R->I1L+g1D	39082
1163	I1R->I5+g1D	39078
1185	I1L->I1R+g1D	39075
1186	I1R->I5+g1D	39073
1201	I1L->I5+I1R+g1D	39577
1213	I1L->g1D	39771
1231	I1R->g1D+I5	39550
1283	I1R->M3L+g1D	39067
1311	I1R->M3L+g1D	39065
1326	I1R->g1D	39063
1328	M3R->pm4+g1D	39420
1337	I1L->M3R+g1D	39424
1489	I6->pm5+g1D	39639
1520	M5->pm5+g1D	39279
1560	M5->pm5+g1D	39275
1584	M5->pm5+g1D	39267

(Continues)

TABLE 1 (Continued)

Section #	Presynaptic neuron -> postsynaptic cells	Synapse ID
1555	M4->pm5+g1VL	39198
1789	NSML->g1VL+I5	39465
1880	M4->pm5+g1VL	39212
1902	NSML->I5+g1VL	39457
1918	M4->pm5+g1VL	39214
1962	M4->pm5+g1VL	39216
2104	NSML->g1VL+I5	39461
2326	NSML->g1VL+unsp.	39738
2422	NSML->g1VL	39744
2429	NSML->g1VL	39740
2436	NSML->pm8+g1VL	39746
1706	M4->pm5+g1VR	39149
1722	M4->pm5+g1VR	39153
1750	M4->pm5+g1VR	39151
1795	M4->pm5+g1VR	39155
1914	NSMR->I5+g1VR	39374
2028	M4->pm5+g1VR	39170
2057	M4->pm5+g1VR	39172
2106	M4->pm5+g1VR	39174
2131	NSML->g1VR+I5	39463

Column one indicates the spatial distribution of the synapses along the length of the gland cells as section numbers (#). The total number of sections of the glands is 2475, counted from the anterior tip of the dorsal gland process (Section 1) to the end of g1VR in the TB (Section 2475). Section thickness is 50 nm. Column two lists the pharyngeal neurons that are presynaptic to the gland cells and to other adjacent output cells as recorded under the synapse IDs given in column three (Bumbarger et al., 2013). All synapses onto the gland cells are represented as simple arrows in Figure 6.

(Bumbarger et al., 2013). In *C. elegans*, the contractile filaments of pm7 are special in that they do not show the usual radial orientation for opening the pharyngeal lumen but are oriented obliquely in anteroposterior direction. When they contract, they exert a specific pull on the grinder (Altun & Hall, 2008), a function that is clearly obsolete in *P. pacificus*.

3.6 | The innervation of the gland cells

Finally, we analyzed the innervation of the *P. pacificus* gland cells. As in *C. elegans*, the dorsal gland is special due to its exposed position at the entrance of the digestive tract and it proves to be highly connected in both species (Bumbarger et al., 2013). The special requirement in *P. pacificus* is that g1D behavior has to be integrated with the respective behavior of the dorsal tooth (activated by pm1) in different food-

source dependent scenarios. The analysis of pharynx connectivity in *P. pacificus* (Bumbarger et al., 2013) has shown that the dorsal gland receives synaptic input from five neurons (M1, I1, M3, I6, M5) in specimen 107 and from three neurons (M1, I1, M3) in specimen 148, whereas the sub-ventral glands in both specimens only receive input from two neurons (M4, NSM) (Figure 6; Tables 1 and 2). As can be seen in Figure 6, the synapses onto the dorsal gland are concentrated on the dorsal side of the process in the region of the corpus. The bulk of synaptic input to the dorsal gland comes from neurons M1 and I1.

TABLE 2 Gland cell innervation of *P. pacificus* specimen 148

Section #	Presynaptic neuron -> postsynaptic cells	Synapse ID
155	M1->pm3D+g1D	27663
204	M1->pm3D+g1D	27665
277	M1->pm3D+g1D	27669
337	M1->pm3D+g1D	27671
587	M1->I3+g1D	27682
664	M1->I3+g1D	27321
722	M1->pm3D+g1D	27684
790	M1->pm3D+g1D	27686
821	M1->pm3D+g1D	27688
984	M1->I5+g1D	19757
1063	M1->I5+g1D	19755
1104	I1L->g1D+e3D	27489
1132	I1L->g1D	27487
1141	I1L->g1D	28322
1173	I1L->g1D+I3	19781
1208	I1L->M3L+g1D	27485
1242	M3R->g1D	27426
1256	M3R->g1D+pm4	27428
1265	I1L->g1D+M3R	27430
1560	M4->g1VL+pm5	28004
1836	M4->pm5+g1VL	28017
2377	NSML->g1VL+bm	28195
2211	NSMR->g1VR+bm	28124
2397	M4->pm7+g1VR	28036
2404	NSMR->g1VR+bm	28126
2428	NSMR->g1VR+bm	28128

Column one indicates the spatial distribution of the synapses along the length of the gland cells as section numbers (#). The total number of sections of the glands is 2456, counted from the anterior tip of the dorsal gland process (Section 1) to the end of g1VR in the TB (Section 2456). Section thickness is 50 nm. Column two lists the pharyngeal neurons that are presynaptic to the gland cells and to other adjacent output cells as recorded under the synapse IDs given in column three (Bumbarger et al., 2013).

M1 is presynaptic to pharyngeal muscle cells pm1, pm2, and pm3 while l1 is the only interneuron with connection to the somatic nervous system. Both neurons are thought to be candidates for the differential regulation of the tooth movement on predatory diet versus bacteria (Bumbarger et al., 2013).

4 | DISCUSSION

This study is part of a long-term effort to investigate the morphological and anatomical basis of the different feeding behaviors of free-living nematodes using *P. pacificus* as a model system characterized by omnivorous and predatory feeding. First, the comparison of the pharyngeal nervous system by comparative connectomics between *C. elegans* and *P. pacificus* had shown the surprising conservation and homology of all 20 neurons constituting the self-contained pharyngeal nervous system (Bumbarger et al., 2013). This study allowed the conclusion that different feeding behaviors result largely from wiring differences in the neuronal networks rather than changes in the cellular composition of the nervous system. Here, we show that the pharyngeal gland cells exhibit a different pattern of evolution. The presence of teeth in *P. pacificus* is associated with the absence of the grinder and the absence of two of the five pharyngeal gland cells found in *C. elegans*. These findings are similar to previous observations in another diplogastrid, *Diplenteron* sp. (Zhang & Baldwin, 1999). Based on the high-resolution molecular phylogeny of Van Megen and coworkers, which indicated that the Diplogastridae are a monophyletic taxon embedded in the paraphyletic Rhabditidae, we speculate that Diplogastridae have lost the grinder and the two gland cells (Van Megen et al., 2009). However, there is evidence for convergence between Cephalobida and Rhabditida in general (Zhang & Baldwin, 2000) so that any evolutionary interpretations with regard to polarity have to be considered with care. Finally, it is interesting to note that the ultra-structural analysis in *P. pacificus* shows a very similar pharyngeal gland cell composition when compared to *Diplenteron* sp., the only other diplogastrid previously investigated (Zhang & Baldwin, 1999). The only observed difference between *Pristionchus* and *Diplenteron* was that in *Diplenteron* sp. the muscle cells pm7 and pm8 are absent, whereas in *P. pacificus* both are still present.

In summary, this comparative morphological analysis provides the basis for functional studies of feeding behavior, in particular the predatory feeding of *P. pacificus* on other nematodes (Lightfoot et al., 2016; Wilecki et al., 2015). Future studies will extend our current knowledge by providing the reconstruction of other parts of the sensory system involved in feeding to ultimately obtain a comprehensive understanding of feeding structures and function.

ACKNOWLEDGMENTS

We are very grateful to Dr. Reza Shahidi for expert help with the preparation of the animated gland cell reconstruction and Bogdan Sieriebriennikov for helpful suggestions and carefully reading the manuscript. The authors declare no conflict of interest.

AUTHOR CONTRIBUTIONS

MR and RJS designed the project. MR performed the reconstruction and MR and RJS wrote the manuscript. The authors declare no conflict of interest.

ORCID

Ralf J. Sommer  <http://orcid.org/0000-0003-1503-7749>

REFERENCES

- Albertson, D. G., & Thomson, J. N. (1976). The pharynx of *Caenorhabditis elegans*. *Philosophical Transactions of the Royal Society of London*, 275B, 299–325.
- Altun, Z. F., & Hall, D. H. (2008). Alimentary System, The Pharynx. In: *C. elegans Atlas*. Coldspring Harbor, NY: Cold Spring Harbor Laboratory Press.
- Avery, D. G., & Thomas, J. H. (1997). Feeding and defecation. In D. L. Riddle, T. Blumenthal, B. J. Meyer, & J. R. Priess (Eds.), *C. elegans* (Vol. II, pp. 679–716). Cold Spring Harbor, NY: Laboratory Press.
- Bento, G., Ogawa, A., & Sommer, R. J. (2010). Co-option of the endocrine signaling module Dafachronic Acid-DAF-12 in nematode evolution. *Nature*, 466, 494–497.
- Bird, A. F., & Bird, J. (1991). *The structure of nematodes*. San Diego, CA: Academic Press.
- Bumbarger, D., & Riebesell, M. (2015). Anatomy and connectivity in the pharyngeal nervous system. In R. J. Sommer (Ed.), *Pristionchus pacificus—A nematode model for comparative and evolutionary biology* (Ch. 12, pp. 353–383). Leiden, NL: BRILL.
- Bumbarger, D. J., Riebesell, M., Rödelsperger, C., & Sommer, R. J. (2013). System-wide circuit reorganization underlying behavioral differences between predatory and bacterial feeding nematodes. *Cell*, 152, 109–119.
- Cardona, A., Saalfeld, S., Schindelin, J., Arganda-Carreras, I., Preibisch, S., Longair, M., ... Douglas, R. J. (2012). TrakEM2 software for neural circuit reconstruction. *PLoS One*, 7, e38011.
- Chiang, J. T., Steciuk, M., Shtonda, B., & Avery, L. A. (2006). Evolution of pharyngeal behaviors and neuronal functions in free-living soil nematodes. *Journal of Experimental Biology*, 209(Pt 10), 1859–1873.
- Chitwood, B. G., & Chitwood, M. B. (1950). *An introduction to nematology*. Baltimore: University Park Press.
- Fürst von Lieven, A. (2002). Functional morphology, origin and phylogenetic implications of the feeding mechanism of *Tylopharynx foetida* (Nematoda: Diplogastrina). *Russian Journal of Nematology*, 10, 183–201.
- Fürst von Lieven, A. (2003). Functional morphology and evolutionary origin of the three-part pharynx in nematodes. *Zoology*, 106, 183–201.
- Fürst von Lieven, A., & Sudhaus, W. (2000). Comparative and functional morphology of the buccal cavity of Diplogastrina (Nematoda) and a first outline of the phylogeny of this taxon. *Journal of Zoological Systematics and Evolutionary Research*, 38, 37–63.
- Herrmann, M., Mayer, W., Hong, R., Kienle, S., Minasaki, R., & Sommer, R. J. (2007). The nematode *Pristionchus pacificus* (Nematoda: Diplogastridae) is associated with the Oriental beetle *Exomala orientalis* (Coleoptera: Scarabaeidae) in Japan. *Zoological Science*, 24, 883–889.
- Kanzaki, N., & Giblin-Davis, R. M. (2015). Diplogastrid systematics and phylogeny. In R. J. Sommer (Ed.), *Pristionchus pacificus—A nematode model for comparative and evolutionary biology* (Ch. 3, pp. 43–76). Leiden, NL: BRILL.

- Kanzaki, N., Ragsdale, E., Herrmann, M., & Sommer, R. J. (2014). Two new and two recharacterized species resulting from a radiation of *Pristionchus* (Nematoda: Diplogasteridae) in Europe. *Journal of Nematology*, 46, 60–74.
- Kieninger, M. R., Ivers, N. A., Rödelsperger, C., Markov, G. V., Sommer, R. J., & Ragsdale, E. J. (2016). The nuclear hormone receptor NHR-40 acts downstream of the sulfatase EUD-1 as part of a developmental plasticity switch in *Pristionchus*. *Current Biology*, 26, 2174–2179.
- Lightfoot J., Wilecki, M., Okumura, M. & Sommer R. J. (2016). Assaying predatory feeding behavior in *Pristionchus* and other nematodes. *J. Vis. Exp.*, 115, e54404.
- Maggenti, A. (1981). *General nematology*. New York: Springer-Verlag.
- Meyer, J. M., Baskaran, P., Quast, C., Susoy, V., Rödelsperger, C., Glöckner, F. O., ... Sommer, R. J. (2017). Succession and dynamics of *Pristionchus* nematodes and their microbiome during decomposition of *Oryctes borbonicus* on La Réunion Island. *Environm. Microbiology*, 19, 1476–1489.
- Morgan, K., McGaughan, A., Witte, H., Bartelmes, G., Villate, L., Herrmann, M., ... Sommer, R. J. (2012). Multi-locus analysis of *Pristionchus pacificus* on La Réunion Island reveals an evolutionary history shaped by multiple introductions, constrained dispersal events, and rare out-crossing. *Molecular Ecology*, 21, 250–266.
- Munn, E. A., & Munn, P. D. (2002). Feeding and digestion. In D. L. Lee (Ed.), *The biology of nematodes* (Ch. 8, pp. 211–232). Boca Raton, London, New York: CRC Press.
- Pires-daSilva, A. (2013, March). *Pristionchus pacificus* protocols. In *WormBook*, (Ed.) *The C. elegans Research Community*, WormBook, doi/10.1895/wormbook.1.114.2.
- Rae, R., Riebesell, M., Dinkelacker, I., Wang, Q., Herrmann, M., Weller, A. M., ... Sommer, R. J. (2008). Isolation of naturally associated bacteria of necromenic *Pristionchus* nematodes and fitness consequences. *Journal of Experimental Biology*, 211, 1927–1936.
- Ragsdale, E. J., Kanzaki, N., & Herrmann, M. (2015). Taxonomy and natural history: The genus *Pristionchus*. In R. J. Sommer (Ed.), *Pristionchus pacificus—A nematode model for comparative and evolutionary biology*. (Ch. 4, pp. 77–120). Leiden, NL: BRILL.
- Ragsdale, E. J., Müller, M. R., Rödelsperger, C., & Sommer, R. J. (2013). A developmental switch coupled to the evolution of plasticity acts through a sulfatase. *Cell*, 155, 922–933.
- Sanghvi, G. V., Baskaran, P., Röseler, W., Sieriebriennikov, B., Rödelsperger, C., & Sommer, R. J. (2016). Life history responses and gene expression profiles of the nematode *Pristionchus pacificus* cultured on *Cryptococcus* yeasts. *PLoS One*, 11, e0164881.
- Seroby, V., & Sommer, R. J. (2017). Developmental systems of plasticity and trans-generational inheritance in nematodes. *Current Opinion in Genetics & Development*, 45, 51–57.
- Seroby, V., Xiao, H., Rödelsperger, C., Namdeo, S., Röseler, W., Witte, H., & Sommer, R. J. (2016). Chromatin remodeling and antisense-mediate up-regulation of the developmental switch gene eud-1 control predatory feeding plasticity. *Nature Communications*, 7, 12337.
- Sommer, R.J. (Ed.). (2015). *Pristionchus pacificus—A nematode model for comparative and evolutionary biology*. Leiden, NL: BRILL.
- Sommer, R. J., Carta, L. K., Kim, S.-Y., & Sternberg, P. W. (1996). Morphological, genetic and molecular description of *Pristionchus pacificus* sp. n. (Nematoda, Diplogasteridae). *Fundamental and Applied Nematology*, 19, 511–521.
- Sommer, R. J., Dardiry, M., Lenuzzi, M., Namdeo, S., Renahan, T., Sieriebriennikov, B., & Werner, M. (2017). The genetics of phenotypic plasticity in nematode feeding structures. *Open Biology*, 7(3), 160332.
- Susoy, V., Ragsdale, E. J., Kanzaki, N., & Sommer, R. J. (2015). Rapid diversification associated with a macroevolutionary pulse of developmental plasticity. *eLIFE*, DOI:10.7554/eLife.05463.002
- Van Megen, H., van den Elsen, S., Holterman, M., Karssen, G., Mooyman, P., Bongers, T., ... Helder, J. (2009). A phylogenetic tree of nematodes based on about 1200 full-length small subunit ribosomal DNA sequences. *Nematology*, 11, 927–950.
- Wilecki, M., Lightfoot, J., Susoy, V., & Sommer, R. J. (2015). Predatory feeding behavior in *Pristionchus* nematodes is dependent on a phenotypic plasticity and induced by serotonin. *Journal of Experimental Biology*, 218, 1306–1313.
- Witte, H., Moreno, E., Rödelsperger, C., Kim, J., Kim, J.-S., Streit, A., & Sommer, R. J. (2015). Gene inactivation using the CRISPR/Cas9 system in the nematode *Pristionchus pacificus*. *Development Genes and Evolution*, 225, 55–62.
- Zhang, Y. C., & Baldwin, J. G. (1999). Ultrastructure of the esophagus of *Diplenteron* sp. (Diplogasterida) to test hypotheses of homology with Rhabditida and Tylenchida. *Journal of Nematology*, 31, 1–19.
- Zhang, Y. C., & Baldwin, J. G. (2000). Ultrastructure of the post-corpus of *Zeldia punctata* (Cephalobina) for analysis of the evolutionary framework of nematodes related to *Caenorhabditis elegans* (Rhabditina). *Proceedings of the Royal Society of London. Series B, Biological Sciences*, 267, 1229–1238.
- Zhang, Y. C., & Baldwin, J. G. (2001). Ultrastructure of the postcorpus of the esophagus of *Teratocephalus lirellus* (Teratocephalida) and its use for interpreting character evolution in Secernentea (Nematoda). *Canadian Journal of Zoology*, 79, 16–25.

SUPPORTING INFORMATION

Additional Supporting Information may be found online in the supporting information tab for this article.

How to cite this article: Riebesell M, Sommer RJ. Three-dimensional reconstruction of the pharyngeal gland cells in the predatory nematode *Pristionchus pacificus*. *Journal of Morphology*. 2017;278:1656–1666. <https://doi.org/10.1002/jmor.20739>